JOURNAL OF MODERN OPTICS, 1992, VOL. 39, NO. 9, 1953–1963

Polarization holographic gratings

Diffraction efficiency of amplitude-phase gratings and their realization in AgCl emulsions

L. NIKOLOVA, T. PETROVA, M. IVANOV, T. TODOROV
and E. NACHEVA

Central Laboratory of Optical Storage and Processing
of Information, Bulgarian Academy of Sciences,
Sofia 1113, P.O. Box 95, Bulgaria

(Received 12 February 1992; revision received 15 May 1992)

Abstract. The photoinduced anisotropy (dichroism and birefringence) in AgCl emulsions is studied as well as the possibility for chemical fixing of this anistropy. A theoretical relation between the diffraction efficiency of amplitude—phase polarization holographic gratings and the photoanisotropy of the recording medium is derived. Based on this relationship an estimation of the properties of the gratings is presented. Polarization holographic gratings with spatial frequencies of 200 to 2000 mm^{-1} and diffraction efficiency up to 1·8% are recorded. The gratings are stable, and do not change in time for more than a year.

1. Introduction

One of the basic applications of holography is in the fabrication of holographic optical elements. The properties of the holographic diffraction gratings are studied and techniques for their production are developed. Thanks to the development of polarization holography [1, 2], a new type of holographic optical element appeared: polarization holographic gratings. These are anisotropic periodical structures, recorded holographically in photoanisotropic materials. Combining the polarizations of the recording light waves, holographic diffraction gratings with predetermined polarization properties can be produced, and some of them have no matches among the conventional optical elements. For example, such are the polarization gratings, recorded in photoanisotropic materials with two waves of equal intensities and orthogonal circular polarizations (left hand and right hand). They split spatially the left hand and right-hand circular component of the light falling on them [3, 4], i.e. they can be employed as circular polarization splitters, or circular polarizers or analysers. A possible application of such an element is in photopolarimeters for simultaneous measurement of Stokes parameters of light [5, 6].

The production of the holographic polarization diffraction gratings depends on the development of efficient and stable photoanisotropic recording materials. So far, the strongest photoanisotropy is exhibited by films of rigid solutions of azodye/polymer [7, 8]. The diffraction efficiency of polarization holographic gratings, recorded in such media, reaches several tens of per cents. However, the recording is unstable with time—at room temperature the gratings decay thermally in several minutes to several days. Considerable photoinduced anisotropy on irradiation with linearly polarized light is observed in AgCl emulsions as well (Weigert-effect) [9–11].

Normally, this process is more or less reversible—when the polarization of light changes, the existing optical axis is destroyed and a new one appears [11]. No method for creating stable polarization holographic grating is known so far.

This work is devoted to investigation of the process of photoinducing optical anisotropy (dichroism and birefringence) in AgCl emulsions, as well as to the opportunity of chemical fixing of this anisotropy.

2. Diffraction efficiency of amplitude-phase holographic polarization gratings

Usually, the diffraction efficiency η of thin holographic gratings is estimated by the amplitude transmission method. As the amplitude transmittance $\mathbf{T}$ has a periodical spatial modulation ($\mathbf{T}=\mathbf{T}(\mathbf{r})$), from its Fourier spectrum the propagation directions and the intensities of the waves diffracted from the grating, can be determined, hence η. However, when the grating is anisotropic, $\mathbf{T}$ is not a scalar, but a tensor quantity. It is necessary to find the relevant Jones matrix $\mathbf{T}_\mathrm{J}$, describing adequately the anisotropy of the element and its spatial modulation. The $\mathbf{T}_\mathrm{J}$ matrix depends on the type of the polarization element produced, i.e. on the polarization of the recording light waves. Here we shall consider the above-mentioned case of a polarization grating, recorded with two waves W_1 and W_2 with orthogonal circular polarizations. The light field resulting from the interaction of such waves is constant in amplitude, and at equal intensities of W_1 and W_2, it has linear polarization, whose direction (polarization angle ϕ) alters periodically in space, depending on the local phase difference 2δ between W_1 and W_2 in accordance with

$$\phi=\delta. \tag{1}$$

In photoanisotropic materials, such light field produces optical axes whose direction changes by the same law. [4] gives Jones matrices of this type of gratings for the case of purely amplitude (due only to dichroism) and purely phase (due only to birefringence) polarization recording. Since the AgCl films we investigate exhibit simultaneously both dichroism and birefringence, here we derive a formula for the diffraction efficiency of amplitude–phase polarization gratings.

The amplitude transmittance at an arbitrary point of the grating in a coordinate system, connected with the direction of the optical axis in this point, is described [12] by the matrix:

$$\mathbf{T}=\exp\left(-\mathrm{i}\varphi_0\right)\exp\left(-\alpha \mathrm{d}\right)\begin{vmatrix}\exp\left(-\Delta\alpha d\right)\exp\left(-\mathrm{i}\Delta\varphi\right) & 0\\ 0 & \exp\left(\Delta\alpha d\right)\exp\left(\mathrm{i}\Delta\varphi\right)\end{vmatrix}, \tag{2}$$

where $\varphi_0=(\varphi_\parallel+\varphi_\perp)/2$, and $\Delta\varphi=(\varphi_\parallel-\varphi_\perp)/2$. $\varphi_\parallel$ is the phase delay of the wave component polarized along the optical axis, $\varphi_\perp$ is the phase delay for the perpendicular component and d is the grating thickness. Similarly, $\alpha=(\alpha_\parallel+\alpha_\perp)/2$ and $\Delta\alpha=(\alpha_\parallel-\alpha_\perp)/2$, where $\alpha_\parallel$ and $\alpha_\perp$ are the amplitude absorption coefficients for the two components.

Since the direction of the recorded optical axes changes in accordance with (1), the matrix $\mathbf{T}_\mathrm{J}$, describing the grating transmission as a whole, can be represented as

$$\mathbf{T}_\mathrm{J}=\mathbf{R}(\delta)\mathbf{T}\mathbf{R}(-\delta), \tag{3}$$

where

$$\mathbf{R}(\delta)=\begin{vmatrix}\cos\delta & \sin\delta\\ -\sin\delta & \cos\delta\end{vmatrix}, \tag{3 a}$$

$$\mathbf{R}(-\delta)=\begin{vmatrix}\cos\delta & -\sin\delta\\ \sin\delta & \cos\delta\end{vmatrix}. \tag{3 b}$$

The substitution into (3) yields

$$\mathbf{T}_\mathrm{J}=\mathbf{T}_0+\mathbf{T}_1 \tag{4}$$

where

$$\mathbf{T}_0=\exp(-\mathrm{i}\varphi_0)\exp(-\alpha d)\,[\cos(\Delta\varphi)\,\mathrm{ch}(\Delta\alpha d)+\mathrm{i}\sin(\Delta\varphi)\,\mathrm{sh}(\Delta\alpha d)]\begin{vmatrix}1 & 0\\ 0 & 1\end{vmatrix}, \tag{5}$$

$$\mathbf{T}_1=\exp(-\mathrm{i}\varphi_0)\exp(-\alpha d)\,[\cos(\Delta\varphi)\,\mathrm{sh}\,\Delta d)+\sin(\Delta\varphi)\,\mathrm{ch}\,(\Delta\alpha d)]\begin{vmatrix}\cos 2\delta & -\sin 2\delta\\ -\sin 2\delta & -\cos 2\delta\end{vmatrix}. \tag{6}$$

It is readily seen that the term $\mathbf{T}_0$ is related to the non-diffracted light wave, directly transmitted through the grating. Its polarization remains unchanged and its amplitude depends on α, $\Delta\alpha$ and $\Delta\varphi$. At $\Delta\alpha=0$ and $\Delta\varphi=0$ it is equal to the amplitude of the light, falling on the grating, attenuated in accordance with the average absorption coefficient α. From the matrix $\mathbf{T}_1$, describing the diffraction from the grating, it may be concluded that, just like in the cases of purely amplitude and purely phase polarization gratings of this type [4], only two diffraction orders exist: ± 1. At that:

(*a*) the polarizations of the two diffracted waves are orthogonal circular—left-hand and right-hand (the polarizations of the recording waves are reconstructed accurately);

(*b*) the intensities I_{+1} and I_{-1} in the plus one and minus one order depend on the polarization of read-out wave W_0 as:

$$I_{+1}/I_{-1}=I_\mathrm{D}/I_\mathrm{L}C, \tag{7}$$

where I_D and I_L are the intensities of the right hand and left hand circular components of W_0, and

$$I_{+1}+I_{-1}=|C|^2 I_0, \tag{8}$$

where $C=[\cos(\Delta\varphi)\,\mathrm{sh}\,(\Delta\alpha d)+\mathrm{i}\sin(\Delta,\varphi)\,\mathrm{ch}\,(\Delta\alpha d)]\exp(-\alpha d)\exp(-\mathrm{i}\varphi)$ and I_0 is the intensity of W_0. When W_0 is with a left-hand circular polarization, $I_{+1}=0$, $I_{-1}=|C|^2 I_0$, and vice versa, for right-hand circular polarization of $W_0, I_{+1}=|C|^2 I_0$, $I_{-1}=0$.

The total diffraction efficiency is

$$\eta=|C|^2. \tag{9}$$

As is evident from (9), at $\alpha=0$, $\Delta\alpha=0$ (lossless medium), the maximum possible value of η is 100%. At $\Delta\varphi=0$ (purely amplitude medium), the maximum theoretical value of η is 25% ($\eta=0{\cdot}25$ at $\alpha>2$ and $\Delta\alpha=\alpha$, i.e. at $\alpha_\parallel=0$ and $\alpha_\perp>4$).

From the above considerations, it is seen that all that is needed to evaluate the efficiencies of polarization holographic gratings is to know the values of the recorded dichroism and birefringence in it.

3. Investigations on photoanisotropy in AgCl emulsions

3.1. *AgCl emulsions*

We investigated layers of fine-grain AgCl emulsions, synthesized by us [11]. The emulsions are prepared by the 'double-jet' method [13] in a medium of inert gelatin. They are washed and prior to coating they contain 25 $\mathrm{g\,l^{-1}}$ AgCl and 40 $\mathrm{g\,l^{-1}}$ gelatin. The layers are coated on a glass substrate. The thickness of the dry layer is 9 μm and the average size of the AgCl microcrystals is 30 nm.

As shown in our previous investigations [11], photoanisotropy is greater in emulsions, chemically sensitized with reducing agents hydrasinhydrochloride ($N_2H_4.2HCl$) and sodium nitrite ($NaNO_2$). These sensitizers are introduced prior to coating. The emulsion layers are designated with A (sensitized with $N_2H_4.2HCl$) and B (sensitized with $NaNO_2$).

In some of the samples the emulsions were also sensitized spectrally for the red region of the spectrum, using rhodacyanin dyes with maximum abosrption at $\approx$650 nm.

3.2. *Technique of photoanisotropic investigations*

The appearance and evolution of the photoinduced anisotropy in all types of films were investigated on the set-up shown in figure 1. The photoprocess is induced with a He–Ne laser beam (1) ($\lambda = 633$ nm) with a linear polarization (vertical). The measuring He–Ne beam (2) has a much lower intensity and its polarization is 45° relative to that of the exciting beam. It passes through the sample and after that Stokes parameters S_i ($i = 0, 1, 2, 3$) and their change with time are measured in real time. This measurement is accomplished with a computerized photopolarimeter (Stokes-meter), described in [14]. The fast and simultaneous measurement of all S_i makes possible the simultaneous tracing of the changes in the average optical density of the samples $D = (D_{\parallel} + D_{\perp})/2$ ($D_{\parallel}$ and $D_{\perp}$ are the optical densities for light polarized parallelly and perpendicularly to the induced optical axis), dichroism $\Delta D = (D_{\parallel} - D_{\perp})$, and birefringence $\Delta n = n_{\parallel} - n_{\perp}$ (the designations of the refractive indices $n_{\parallel}$ and $n_{\perp}$ are analogous). As described in [14], at such experimental geometry, D, ΔD and Δn can be evaluated by the measured values of S_i in accordance with

$$D = (1/2)\lg[S_0^2/(S_0^2 - S_1^2)], \tag{10}$$

$$\Delta D = \lg[(S_0 - S_1)/(S_0 + S_1)]. \tag{11}$$

$$\Delta n = (\lambda/2\pi d)\,\mathrm{arctg}\,(S_3/S_2), \tag{12}$$

where λ is the wavelength of the measuring light in free space.

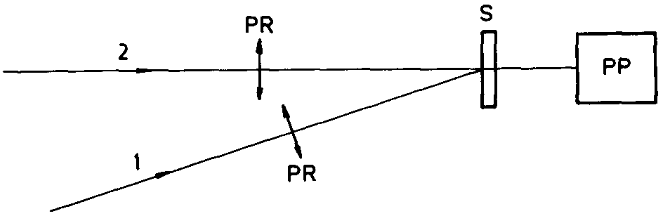

Figure 1. Experimental set-up for measurement of the photoinduced anisotropy: 1—exiting laser beam, 2—measuring beam, PR—polarization rotators, S—sample, PP—photopolarimeter.

Two types of experiments, involving photoinduction of anisotropy in the samples, were carried out:

(*a*) preliminary illumination of the layers with u.v. light in order to create an absorption band in the visible region with subsequent irradiation with a linearly polarized He–Ne beam (a standard way of observing Weigert effect in AgCl emulsions [9, 10, 11]);

(*b*) direct irradiation with a linearly polarized He–Ne laser beam of spectrally sensitized samples (a method of inducing Weigert effect, suggested in [15]).

3.3. *Experimental results*

Figure 2 illustrates the results from the measurement of the changes in D, ΔD and anisotropic phase difference $\Delta\varphi = (2\pi/\lambda)\Delta nd$, induced by the linearly polarized He–Ne laser beam in spectrally non-sensitized samples, illuminated in advance with u.v. light to saturation. Curves A are for samples of type A, and curves B—for samples of

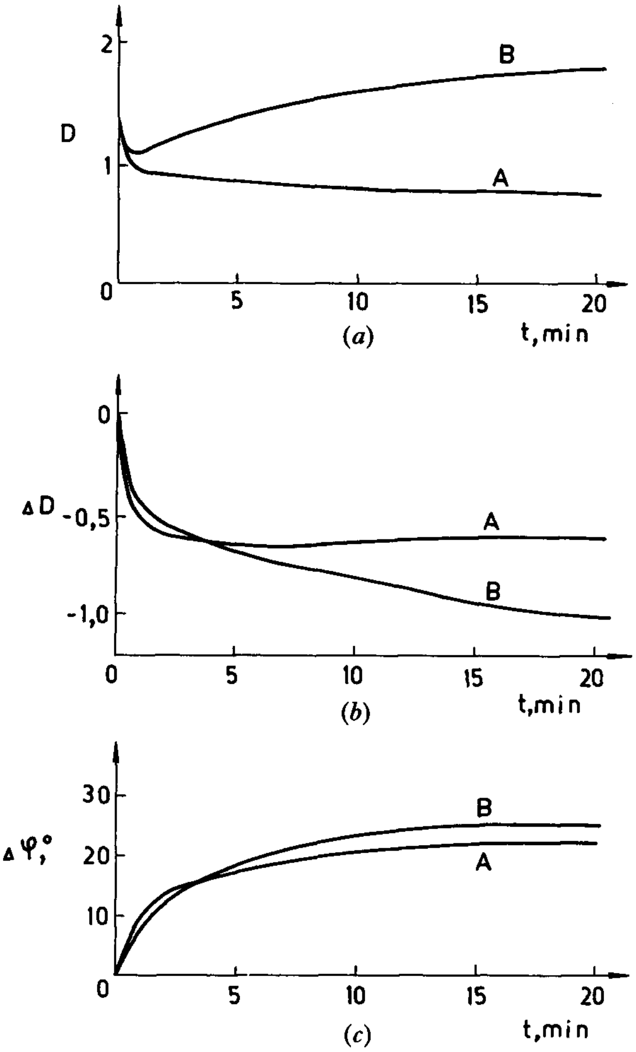

Figure 2. The changes in: mean optical density D (figure 2 (*a*)), dichroism ΔD (figure 2 (*b*)) and anisotropic phase difference $\Delta\varphi$ (figure 2 (*c*)), induced by a linearly polarized He–Ne laser beam (300 mW cm^{-2}) in films previously darked with u.v. light. The curves A and B correspond to samples of types A and B.

type *B*. The initial optical densities of the films at $\lambda = 630$ nm are 1·3. The laser beam power was 300 mW cm^{-2}. Its action brings about considerable bleaching in the samples of type *A* (figure 2 (*a*), curve *A*). At the same time, considerable anisotropy is induced both in the absorption and the refractive index (figure 2 (*b*, *c*), curve *A*). ΔD and Δn ($\Delta\varphi$) become saturated relatively rapidly with time. The behaviour of samples *B* differs from that of samples *A*. Following a weak initial decrease, the average optical density *D* increases and reaches values that cannot be obtained in the preliminary illumination. This is accompanied by a very strong dichroism, growing incessantly while the He–Ne beam is switched on (20 min). The birefringence, induced in both types of samples, is practically the same.

Figure 3 shows the results from the measurement of the changes in *D*, ΔD and $\Delta\varphi$, induced in spectrally sensitized samples of types *A* and *B* by direct illumination with a linearly polarized He–Ne laser beam (without preliminary illumination). The laser beam power is like before 300 mw cm^{-2}. The comparison between the curves reveals that the initial rate of growth of the average optical density *D*, dichroism ΔD

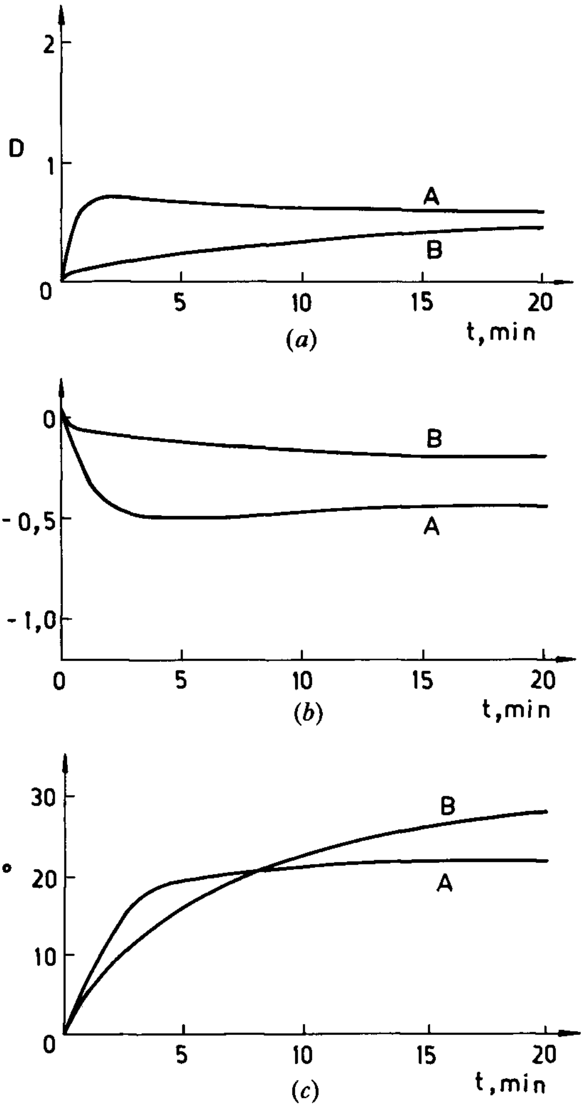

Figure 3. As in figure 2 but for spectrally sensitized samples of type *A* and *B*.

and anisotropic phase delay $\Delta\varphi$, caused by birefringence, is much higher in the samples of type *A*. After several minutes of irradiation they become saturated. The photoinduced changes in the samples of type *B* are much slower. However, on longer irradiation they continue to increase and the birefringence exceeds that in samples *A*.

4. Fixing of the photoanisotropy in AgCl emulsions

If the AgCl emulsions are to be used for polarization optical elements, the photoinduced anisotropy in them must be fixed. Fixing of photographic silver-halide materials is a well known process. However, our experiments showed that conventional fixing methods with sodium thiosulphate in this case are inappropriate. Because of their small size, the photolytic Ag specks have strong solubility and a great part of them dissolve in the fixing agent, leading to a strong decrease in the photoinduced anisotropy. In order to confine the photoanisotropic decay in the fine-grain AgCl emulsion during fixing, the solubility of AgCl microcrystals must be increased and the solubility of the photolytic Ag specs must be decreased. The solubility of moderately soluble compounds like AgCl can be increased considerably by the addition of substances, capable of binding one of the ions in a soluble complex. The addition of NH_3 results in binding Ag^+ in soluble $Ag\,(NH_3)_2^+$, diminishing the concentration of the free Ag^+. The product of the activities of the free Ag^+ and Cl^- ions becomes smaller than the solubility product of AgCl and in order to restore the equilibrium additional quantity of AgCl is dissolved.

The solubility of the photodichroic Ag specks can be decreased by adsorbing a silver salt, less soluble than AgCl, on the surface. The merkaptane Ag salts have about six orders of magnitude smaller solubility product than AgCl [13]. The fixing composition was chosen such that phenilmercaptotetrazole (PMT) or 2-Mercaptobenzothiazole (MBT) are adsorbed on the surface of the Ag specks, and AgCl is dissolved in an ammonia complex in water-alcohol medium.

Table 1 shows the values of *D*, ΔD and $\Delta\varphi$, measured after fixing the samples whose photoanisotropy is shown in figures 2 and 3. For comparison, the corresponding final values before fixing are also given.

The general conclusion from the results is that fixing causes a decrease in the photoinduced values of *D*, ΔD and $\Delta\varphi$ in all samples. The decrease in $\Delta\varphi$ is relatively weak. More pronounced is the general bleaching of the layers and the decrease in dichroism ΔD. The ratio $\Delta D/D$ also decreases, stronger in the samples of type *A* than in the samples of type *B*.

Table 1. The values of the mean optical density *D*, dichroism ΔD and anisotropic phase delay $\Delta\varphi$ of samples of types *A* and *B* after a 20 min exposition to a laser beam, 300 mW cm^{-2}, before and after chemical fixing. (1) spectrally non-sensitized samples, previously darkened to optical density 1·3; (2) spectrally sensitized for 630 nm samples.

		Before fixing			After fixing		
		D	ΔD	$\Delta\varphi$ (deg)	*D*	ΔD	$\Delta\varphi$ (deg)
(1)	*A*	0·74	−0·61	23·4	0·43	−0·09	18·0
	B	1·82	−1·05	26·1	0·82	−0·36	23·0
(2)	*A*	0·58	−0·44	22·1	0·28	−0·04	15·5
	B	0·46	−0·20	28·1	0·33	−0·11	22·0

5. Estimation of the diffraction efficiency of polarization gratings in AgCl emulsions and their realization

From the measured values of the photoinduced changes in the optical constants of AgCl emulsion layers, and using the formulae, derived in Section 2, an estimate was made of the diffraction efficiency of polarization diffraction gratings. Figure 4 illustrates the increase in the diffraction efficiency η, calculated in accordance with (9), for the two types of emulsion layers at $\lambda = 630\,\mathrm{nm}$ when the recording is accomplished with a He–Ne laser in spectrally non-sensitized emulsions after preliminary illumination with u.v. light. Figure 5 shows similar curves, corresponding to direct recording in sensitized emulsions. In both figures, curves 1 represent the calculated values of the total diffraction efficiency, and curves 2—only the amplitude component of the recording (in formula (9) $\Delta\varphi$ is set to zero). It is seen that despite the considerable photoanisotropy, the values of η are substantially lower than the theoretical maximum. This is due to the considerable absorption of the films at relatively low dichroism (in all samples ΔD is lower than D).

It is interesting to note that in the layers, darkened in advance, the recording is primarily amplitude modulation. The same holds true for the spectrally sensitized layers of type *A*. The recording has a noticeable phase component in the spectrally sensitized layers of type *B*.

Table 2 shows the values of η for the two types of media, calculated from the measured values of D, ΔD and $\Delta\varphi$ before and after fixing (from table 1). It is seen that fixing affects in different ways the amplitude and phase component of the recording. In one of the cases, fixing causes an increase in η. This is due to the strong decrease in the average absorption during fixing.

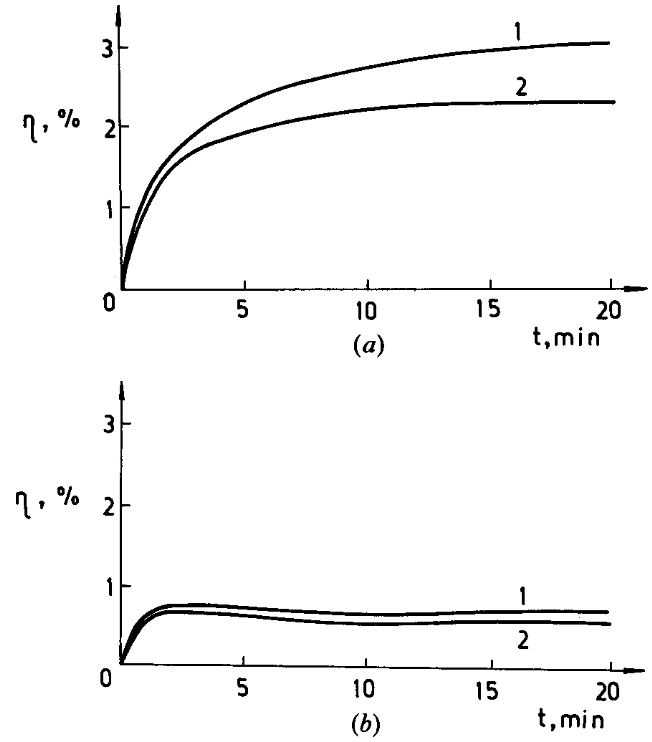

Figure 4. Dependence of the diffraction efficiency η (calculated values) on the recording time for samples previously darkened with u.v. light. Figure 4 (*A*) and 4 (*B*) correspond to samples of types *A* and *B*. The curves 1 correspond to the total diffraction efficiency and the curves 2 only to the amplitude part of η.

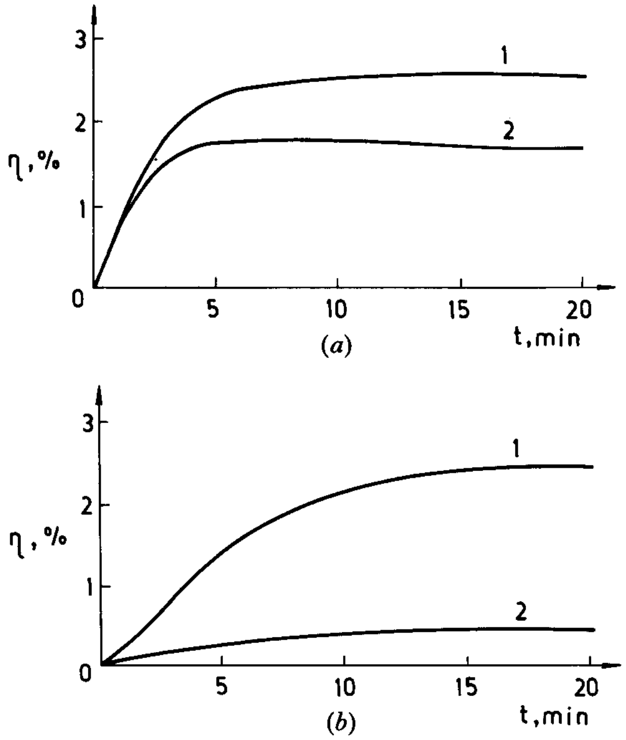

Figure 5. As in figure 4 but for spectrally sensitized samples.

Table 2. The values of the diffraction efficiency of the polarization holographic diffraction grating (η) and the amplitude part of η (η_0) calculated in accordance to (8) and (9) for the corresponding values of D, ΔD and $\Delta\varphi$ given in table 1 for samples of types A and B, before and after chemical fixing. (1) spectrally non-sensitized samples, (2) spectrally sensitized for 630 nm samples.

		Before fixing		After fixing	
		η [%]	η_0[%]	η [%]	η_0[%]
(1)	A	3·17	2·42	1·02	0·10
	B	0·65	0·57	1·26	0·66
(2)	A	2·70	1·70	0·98	0·03
	B	2·50	0·46	1·90	0·19

Figure 6 shows the relationship between the values of η, calculated from (9), and the intensity of the He–Ne laser beam,for the case of direct irradiation with polarized light in spectrally sensitized samples. The irradiation duration is one and the same for all intensities (20 min). Curve A corresponds to samples of type A, and curve B to samples of type B. The difference between the two curves indicates that the sensitivity of layers A is much greater—at low intensities of the exciting light, the recording in them is several times more efficient. At higher intensity values, η_A and η_B tend to become equal. Figure 7 shows similar relationships after fixing.

The spectrally sensitized emulsions of type A were used for recording polarization holographic gratings with two waves with orthogonal circular polarizations at

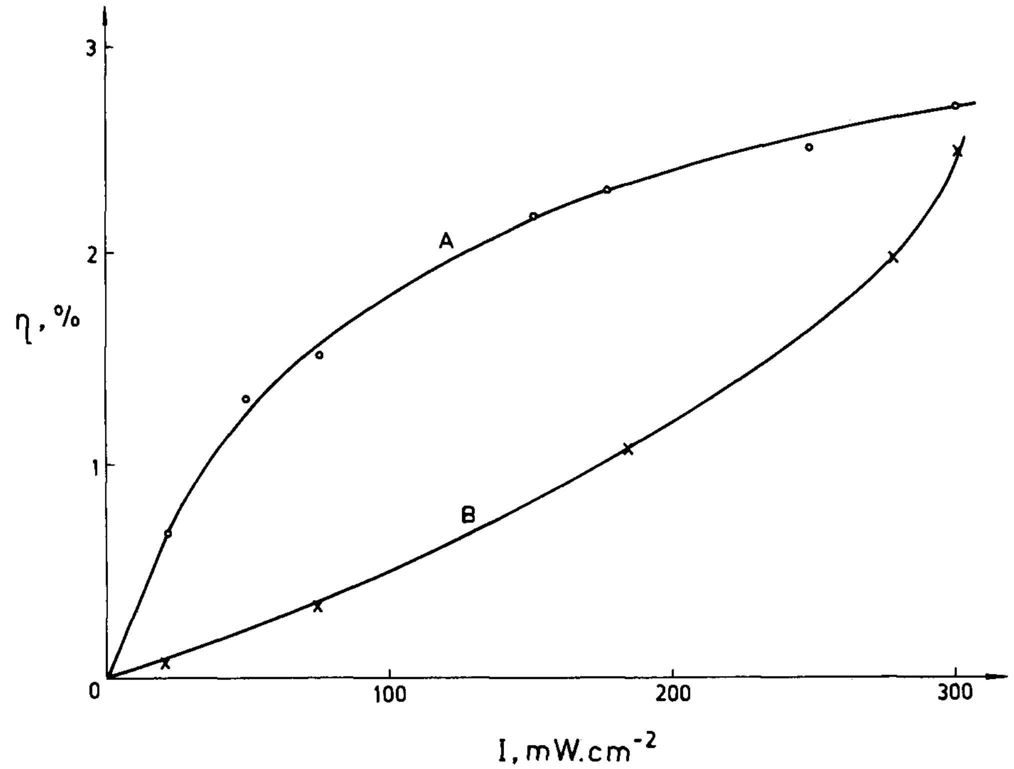

Figure 6. Dependence of η on the recording light intensity at direct recording, 20 min, on spectrally sensitized samples, before chemical fixing. Curves *A* and *B* correspond to samples *A* and *B*.

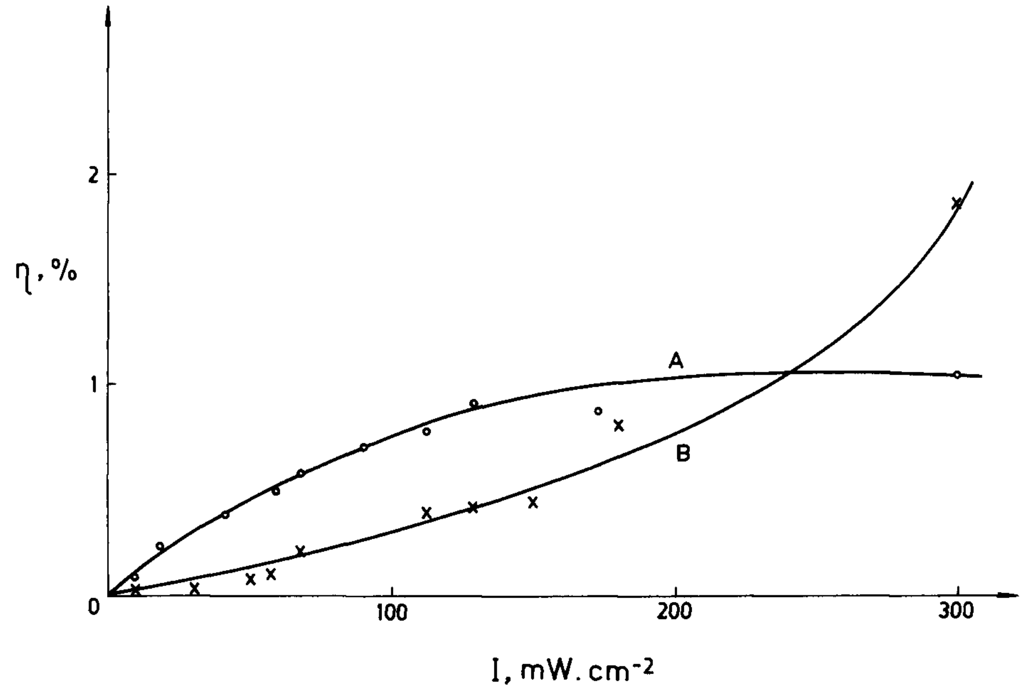

Figure 7. The same dependence after the chemical fixing of the recording.

$\lambda = 633$ nm. The spatial frequency of the gratings was altered from 200 to 2000 mm^{-1} and no influence on the recording efficiency was observed. After fixing, the gratings have diffraction efficiencies 1·8% in an area of 7 mm^2 and 0·6% in an area of 1·5 cm^2. The decrease in η for the larger gratings is merely a consequence of the decrease in the energy density (300 mW cm^{-2} and 40 mW cm^{-2} respectively). The gratings are stable and do not change for more than a year.

6. Conclusions

A method of recording stable polarization holographic gratings in fine-grain sensitized AgCl emulsion layers has been found. From the two types of chemical sensitizers used, hydrasinhydrochloride turned out to be more appropriate (layers of type A) for large-area gratings. This type of media permit grating recording at lower light intensity and shorter exposure times, which is important in view of vibrations during the holographic recording.

References

[1] Kakichashvili, Sh. D., 1989, *Polarization Holography* (Nauka) (in Russian).

[2] Kakichashvili, Sh. D., 1982, *Vestnik AN USSR*, No. 7, 51 (in Russian).

[3] Kakichashvili, Sh. D., 1981, *Pisma Zh. Tekh. Fiz.*, **7**, 239.

[4] Nikolova, L., and Todorov, T., 1984, *Optica Acta*, **31**, 579.

[5] Nikolova, L., Todorov, T., Sharlandjiev, P., and Stoyanov, St., 1989, *Proceedings SPIE*, **1189**, Holography '89, 280.

[6] Todorov, T., and Nikolova, L., 1992, *Optics Lett.*, **17**, 358.

[7] Kakichashvili, Sh. D., and Shataline, I. D., 1986, *Pisma Zh. Tekh. Fiz.*, **12**, 277.

[8] Todorov, T., Nikolova, L., and Tomova, N., 1984, *Appl. Optics*, **23**, 4583.

[9] Weigert, F., 1920, *Ann. Phys.*, **63**, 682.

[10] Jonathan, J. M., and May, M., 1980, *Appl. Optics*, **20**, 2061.

[11] Petrova, Tz., Pangelova, N., Nikolova, L., and Todorov, T., 1985, *J. Imag. Sci.*, **29**, 238.

[12] Azzam, R. M. A., and Bashara, N. M., 1977, *Ellipsometry and Polarized Light* (North-Holland).

[13] James, T., 1977, *The Theory of the Photographic Process*, fourth ediction (Macmillan).

[14] Nikolova, L., Todorov, T., Sharlandjiev, P., and Stoyanov, St., 1992, *Appl. Optics*, (to be published).

[15] Matulis, L., and Yanuchevicheva, J., 1957, *Zh. Nauch. Prikl. Photigr. Kimenatogr.*, **2**, 91 (in Russian).